SHOCK, Vol. 38, No. 2, pp. 177–185, 2012

DIETARY PHOSPHATIDYLCHOLINE SUPPLEMENTATION ATTENUATES INFLAMMATORY MUCOSAL DAMAGE IN A RAT MODEL OF EXPERIMENTAL COLITIS

Tamás Kovács,[*] Gabriella Varga,[†] Dániel Érces,[†] Tünde Tőkés,[†] László Tiszlavicz,[‡] Miklós Ghyczy,[†] Mihály Boros,[†] and József Kaszaki[†]

**Department of Paediatrics, [†]Institute of Surgical Research, and [‡]Department of Pathology, Faculty of Medicine, University of Szeged, Szeged, Hungary*

Received 12 Mar 2012; first review completed 26 Mar 2012; accepted in final form 1 May 2012

ABSTRACT—This study was designed to follow the time course of inflammatory activation in a rodent model of 2,4,6-trinitrobenzenesulfonic acid (TNBS)–induced colitis. We hypothesized that oral phosphatidylcholine (PC) pretreatment regimens may influence leukocyte-mediated microcirculatory reactions in this condition. In series I, Wistar rats were monitored 1 day after colitis induction (n = 24), and in series II (n = 24) on day 6 following a TNBS enema. The PC-pretreated animals received a 2% PC-enriched diet for 6 days before the TNBS enema (series I), or for 3 days before and 3 days after TNBS treatment (series II). The macrohemodynamics, serosal microcirculation (visualized by intravital videomicroscopy), colonic xanthine oxidoreductase, myeloperoxidase and nitric oxide end products, and changes in proinflammatory cytokine levels in plasma were measured. The mucosal structural injury was monitored *in vivo* by means of confocal laser scanning endomicroscopy. The TNBS enema induced a systemic hyperdynamic circulatory reaction with increased serosal capillary blood flow and significantly elevated colonic inflammatory enzyme activities, levels of nitric oxide production, and cytokine concentrations. Acute colitis caused disruption of the capillary network, whereas the morphologic damage was less severe in series II. The PC pretreatment protocols led to significant decreases in the serosal hyperemic reaction, the cytokine levels, and the inflammatory enzyme activities. The objective signs of tissue damage were reduced in both series, and the number of mucus-producing goblet cells in the resolving phase of colitis was increased. Dietary PC efficiently decreases the cytokine-mediated progression of inflammatory events and preserves the microvascular structure in the large intestine.

KEYWORDS—Colitis, fluorescence confocal laser scanning endomicroscopy, inflammation, microcirculation, phosphatidylcholine

INTRODUCTION

Inflammatory bowel diseases (IBDs) are chronic remitting and relapsing disorders of the gastrointestinal (GI) tract with undetermined etiology and without specific therapy. The currently used conservative approaches involve attempts to block the inflammatory activation or to prevent the relapses with local and systemic anti-inflammatory or immunomodulatory agents (1). In this framework, dietary manipulations are of particular interest, as the nutrition can offer appropriate ways via which to intervene in the GI inflammatory cascade in a preventive manner (2). In this respect, many published data have suggested that exogenous phosphatidylcholine (PC) could offer a possible means of targeting the inflammatory reaction in the GI tract. Phosphatidylcholine is a ubiquitous membrane phospholipid, but a number of studies have demonstrated that PC treatment alleviates the consequences of inflammation and ischemia in different organs and experimental models (3–9). Furthermore, it has been reported that the PC content is decreased in the mucus of patients with ulcerative colitis (10) and that local increases in the mucus PC level are accompanied by decreased inflammatory activity.

Our primary aim was to follow the time course of inflammatory activity in the large intestine during the acute (early) and subacute (resolving) phases of experimental colitis. We used the hapten 2,4,6-trinitrobenzenesulfonic acid (TNBS), which is widely administered to rodents for IBD pathomechanism studies and to test new therapeutic and pharmacologic possibilities. This model shares many similarities with clinical IBD, with rising levels of the proinflammatory cytokines tumor necrosis factor α (TNF-α) and interleukin-6 (IL-6) (11), tissue granulocyte accumulation, elevated extents of nitric oxide (NO) and peroxynitrite formation (12, 13), weight loss (14), and mucosal barrier damage (15). As a consequence of inflammation, a mucosal microcirculatory dysfunction develops with leukocyte recruitment and extravasation, which is followed by the formation of large amounts of oxygen radicals (16) and oxidative stress. Nevertheless, the pathophysiological consequences of colitis are time-dependent, and inflammatory or morphologic changes in the acute stage are not directly relevant to later phases (17). To date, however, there have been no *in vivo* studies in which the early and later microcirculatory effects of TNBS administration have been characterized and compared in the same setup. Likewise, the effects of dietary PC in the acute and subacute phases of colitis have not been mapped so far. Thus, our secondary aim was to investigate the mechanism of the anti-inflammatory effects of PC, with special emphasis on microcirculatory and morphologic analyses. The recent development of a fiberoptic confocal endomicroscope

Address reprint requests to Mihály Boros, MD, PhD, Institute of Surgical Research, University of Szeged, PO Box 427, H-6701 Szeged, Hungary. E-mail: boros.mihaly@med.u-szeged.hu.

T.K. and G.V. contributed equally to this work.

The study was supported by Hungarian Science Research Fund OTKA K75161, ETT 442/2009, TAMOP-4.2.2A.

The authors have no conflicts of interests.

DOI: 10.1097/SHK.0b013e31825d1ed0

permits potential applications for the noninvasive monitoring of dynamic processes (18) and offers the possibility of acquiring precise *in vivo* data for histological analysis. The sectioning, fixation, and embedding of tissues and postmortem artifacts can be avoided, and a three-dimensional optical biopsy can be obtained without physical disruption of the epithelial layer (19).

MATERIALS AND METHODS

Animals

The experimental protocol was approved by the Ethical Committee for the Protection of Animals in Scientific Research at the University of Szeged and followed the National Institutes of Health guidelines for the care and use of experimental animals. The experiments were performed on 48 male Sprague-Dawley rats (280–320 g) housed in plastic cages in a thermoneutral environment (21°C ± 2°C) with a 12-h dark-light cycle. The animals, fed on a normal diet with tap water *ad libitum*, were randomly allocated into one or other of six experimental groups according to the feeding protocols.

Experimental protocol

In the first part of the studies, 24 animals were randomly allocated into three groups. Group 1 (n = 8) served as sham-operated controls; the animals received enemas with the solvent for TNBS (25% ethanol in a total volume of 0.25 mL) and were nourished with standard laboratory chow. The group 2 animals (n = 8) were kept on a standard laboratory diet for 6 days, and colitis was induced then with a TNBS enema. In group 3 (n = 8), the animals were fed with a special diet (Ssniff Spezialdiäten, Soest, Germany) containing 2% PC (1,2-diacylglycero-3-phosphocholine, R45, Lipoid GmbH, Ludwigshafen, Germany) for 6 days before the TNBS enema. In these groups, the experiments were started with baseline hemodynamic measurements 1 day after TNBS induction.

The experimental setup was identical on day 6 in the subacute phase of TNBS colitis. Group 4 (n = 8), nourished with standard laboratory chow, served as the sham-operated group; the enema was performed with the solvent of TNBS. In group 5 (n = 8), colitis was induced with the TNBS enema 6 days before the measurements, and these animals were fed with standard laboratory chow. In group 6 (n = 8), colitis was induced with the TNBS enema 6 days before the start of the observations, and the animals were fed with the 2% PC-enriched diet for 3 days before and 3 days after the TNBS enema. The hemodynamic measurements were started 6 days following the TNBS enema.

In series I, the animals in groups 1 to 3 were anesthetized 1 day after the TNBS enema; in series II, groups 4 to 6 were anesthetized 6 days after colitis induction. Surgery was performed to allow registration of the hemodynamic parameters at 1-h intervals for 6 h (cardiac output [CO] data were measured only at the end of the experiments). Intravital videomicroscopy was performed at the end of the experiments to visualize the serosal microcirculation 3 cm distal from the cecum. In addition, fluorescence confocal endomicroscopy was performed to examine the microvasculature and morphologic changes of the mucosa of the distal colon, and full-thickness tissue samples and venous blood samples were taken to determine the biochemical changes in the colon and plasma.

Induction of colitis

Colonic inflammation was induced by intracolonic administration of TNBS (40 mg/kg in 0.25 mL of 25% ethanol) through an 8-cm-long soft plastic catheter under transient diethylether anesthesia (14). In the sham-operated groups, only the vehicle for TNBS was administered. The animals were deprived of food, but not water, for 12 h before the enemas.

Surgical preparation

The animals were anesthetized with sodium pentobarbital (50 mg/kg body weight i.p.) 1 or 6 days after the enema and placed in a supine position on a heating pad. Tracheostomy was performed to facilitate spontaneous breathing, and the right jugular vein was cannulated with PE-50 tubing for fluid administration and Ringer's lactate infusion (10 mL/kg per hour) during the experiments. A thermistor-tip catheter (PTH-01; Experimetria Ltd, Budapest, Hungary) was positioned into the ascending aorta through the right common carotid artery to measure the CO by a thermodilution technique. The right femoral artery was cannulated with PE-40 tubing for mean arterial pressure (MAP) and heart rate (HR) measurements.

Hemodynamic measurements

Pressure signals (BPR-02 transducer; Experimetria Ltd) were measured continuously and registered with a computerized data-acquisition system (Experimetria Ltd). Cardiac output was detected by a thermodilution technique, using a SPEL Advanced Cardiosys 1.4 computer (Experimetria Ltd). Gases in arterial blood samples were measured with a blood gas analyzer (AVL Compact 2, Graz, Austria).

Intravital videomicroscopy measurements

The intravital orthogonal polarization spectral imaging technique (Cytoscan A/R; Cytometrics, Philadelphia, Pa) was used for continuous visualization of the microcirculation of the colon serosa. This technique uses reflected polarized light at the wavelength of the isobestic point of oxyhemoglobin and deoxyhemoglobin (548 nm). Because polarization is preserved in reflection, only photons scattered from a depth of 200 to 300 μm contribute to the image formation. A 10× objective was introduced into the intestinal lumen, and the microscopic images were recorded with an S-VHS video recorder (Panasonic AG-TL 700; Matsushita Electric Ind Co Ltd, Osaka, Japan). Microcirculatory evaluation was performed off-line by frame-to-frame analysis of the videotaped images. The changes in capillary red blood cell velocity (RBCV, μm/s) in the postcapillary venules were determined in three separate fields by means of a computer-assisted image analysis system (IVM Pictron, Budapest, Hungary). All microcirculatory evaluations were performed by the same investigator.

Preparation of colon biopsies

Colon biopsies kept on ice were homogenized in phosphate buffer (pH 7.4) containing 50 mM Tris-HCl (Reanal, Budapest, Hungary), 0.1 mM EDTA, 0.5 mM dithiothreitol, 1 mM phenylmethylsulfonyl fluoride, 10 μg/mL soybean trypsin inhibitor, and 10 μg/mL leupeptin (Sigma-Aldrich GmbH, Munich, Germany). The homogenate was centrifuged at 4°C for 20 min at 24,000*g*, and the supernatant was loaded into centrifugal concentrator tubes (Amicon Centricon-100; 100,000-molecular-weight cutoff ultrafilter, Millipore Corporation, Bedford, MA). The activity of xanthine oxidoreductase (XOR) was determined in the ultrafiltered supernatant, whereas that of myeloperoxidase (MPO) was measured on the pellet of the homogenate.

Xanthine oxidoreductase enzyme activity

The XOR activity was determined in the ultrafiltered, concentrated supernatant by a fluorometric kinetic assay based on the conversion of pterine to isoxanthopterine in the presence (total XOR) or absence (xanthine oxidase activity) of the electron acceptor methylene blue (9).

Tissue MPO activity

The activity of MPO as a marker of tissue leukocyte infiltration was measured on the pellet of the homogenate (9). Briefly, the pellet was resuspended in K_3PO_4 buffer (0.05 M; pH 6.0) containing 0.5% hexa-1,6-*bis*-decyltriethylammonium bromide. After three repeated freeze-thaw procedures, the material was centrifuged at 4°C for 20 min at 24,000*g*, and the supernatant was used for MPO determination. Subsequently, 0.15 mL of 3,3′,5,5′-tetramethylbenzidine (dissolved in dimethyl sulfoxide; 1.6 mM) and 0.75 mL of hydrogen peroxide (dissolved in K_3PO_4 buffer; 0.6 mM) were added to 0.1 mL of the sample. The reaction led to the hydrogen peroxide–dependent oxidation of tetramethylbenzidine, which could be detected spectrophotometrically at 450 nm (UV-1601 spectrophotometer; Shimadzu, Kyoto, Japan). Myeloperoxidase activities were measured at 37°C; the reaction was stopped after 5 min by the addition of 0.2 mL of H_2SO_4 (2 M), and the resulting data were referred to the protein content.

Plasma nitrite/nitrate level measurements

The levels of plasma nitrite/nitrate (NO_x), stable end products of NO were measured by the Griess reaction. This assay depends on the enzymatic reduction of nitrate to nitrite, which is then converted into a colored azo compound that is detected spectrophotometrically at 540 nm.

Measurement of plasma TNF-α and IL-6

Blood samples (0.5 mL) were taken from the inferior caval vein into precooled, heparinized (100 U/mL) polypropylene tubes, centrifuged at 1,000*g* at 4°C for 30 min and then stored at −70°C until assay. Plasma TNF-α concentrations were determined in duplicate by means of a commercially available enzyme-linked immunosorbent assay (Quantikine ultrasensitive enzyme-linked immunosorbent assay kit for rat TNF-α; Biomedica Hungaria Kft, Budapest, Hungary). The minimum detectable level was less than 5 pg/mL, and the inter-assay and intra-assay coefficients of variation were less than 10%.

Plasma IL-6 concentrations were measured with a commercially available enzyme-linked immunosorbent assay (Quantikine ultrasensitive enzyme-linked immunosorbent assay kit for rat IL-6; Biomedica Hungaria Kft). The minimum detectable dose of rat IL-6 was in the range 14 to 36 pg/mL.

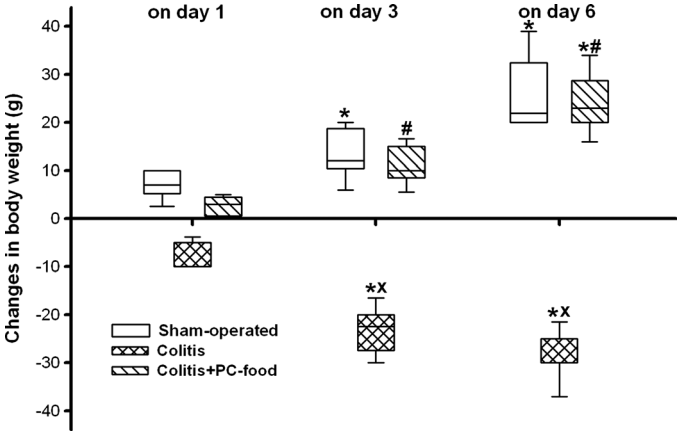

FIG. 1. **Changes in body weight between days 1 and 6 in the sham-operated (white box), colitis (checked white box), and PC-pretreated colitis (striped white box) groups**. The plots demonstrate the median (horizontal line in the box) and the p25 (lower whisker) and p75 (upper whisker). $^{*}P < 0.05$ within groups versus baseline values, $^{x}P < 0.05$ between groups and sham-operated group, $^{\#}P < 0.05$ between PC-pretreated groups and colitis group.

In vivo *detection of tissue damage*

The extent of mucosal damage of the distal colon was evaluated by means of fluorescence confocal laser scanning endomicroscopy (Five1; Optiscan Pty Ltd, Melbourne, Victoria, Australia) developed for *in vivo* histology. The analysis was performed twice, separately by two investigators (T.K. and G.V.). The mucosal surface of the distal colon 8 cm proximal to the anus was surgically exposed and laid flat for examination. The microvascular structure was recorded after the i.v. administration of 0.3 mL of fluorescein isothiocyanate–dextran (FITC-dextran, 150 kd, 20 mg/mL solution dissolved in saline; Sigma-Aldrich Chem, St. Louis, MO). The objective of the device was placed onto the mucosal surface of the descending colon, and confocal imaging was performed 5 min after dye administration (1 scan/image; 1,024 × 512 pixels and 475 × 475 μm per image). The changes in the mucosal architecture were examined following topical application of the fluorescent dye acridine orange (Sigma-Aldrich Inc, St Louis, Mo). The surplus dye was washed off the mucosal surface of the colon with saline 2 min before imaging.

Nonoverlapping fields of active areas of disease were processed in TNBS-treated animals and compared with the samples of PC-treated or control groups by using a semiquantitative scoring system. We used four criteria: (I) the structure of the microvessels (0 = normal; 1 = dye extravasation, but the vessel structure recognizable; 2 = destruction, and the vessel structure unrecognizable); (II) crypt denudation (0 = no denudation; 1 = at least one area without a recognizable crypt structure per field of view; 2 = more than one area without a recognizable crypt structure per field of view, or more than 30% of the field covered by denuded crypts); (III) edema (0 = no edema, 1 = moderate epithelial swelling, 2 = severe edema); and (IV) epithelial cell outlines (0 = normal, clearly, well-defined outlines; 1 = blurred outlines; 2 = lack of normal cellular contours). In each field of view, the number of goblet cells was counted, and the ratio relative to the number of visualized glands was calculated (number of goblet cells / number of glands).

Conventional histopathological analysis

Full-thickness colon biopsies taken at the end of the experiments were analyzed in each group. The tissue was fixed in 6% buffered formalin, embedded in paraffin, cut into 4-μm-thick sections, and stained with hematoxylin-eosin. The coded sections were evaluated by an independent specialist in histopathology (L.T.). The infiltration of leukocytes was detected, and the severity of tissue damage was compared with that in the control group by using a modification of semiquantitative scoring system of Riley et al. (20). The grading was performed with the following criteria: (*a*) acute inflammatory cell infiltration of the lamina propria with polymorphonuclear (PMN) cells (0–3); (*b*) crypt abscess (0–3); (*c*) mucin depletion (0–3); (*d*) surface epithelial integrity (0–3); (*e*) chronic inflammatory cell infiltrate, round cells in the lamina propria (0–3); (*f*) crypt architectural irregularities (0–3); (*g*) transmural lesion or the lesions affected the lamina propria only (0–1); (*h*) diffuse or focal lesion (0–1).

Statistical analysis

Data analysis was performed with a statistical software package (SigmaStat for Windows; Jandel Scientific, Erkrath, Germany). Friedman repeated-measures analysis of variance on ranks was applied within groups. Time-dependent differences from the baseline (Fig. 1) for each group were assessed by Dunn method. Differences between groups were analyzed with Kruskal-Wallis one-way analysis of variance on ranks, followed by Dunn method for pairwise multiple comparisons. In the figures, median values and 75th (p75) and 25th (p25) percentiles are given; $P < 0.05$ was considered statistically significant.

RESULTS

Estimation of the severity of colitis

We estimated the severity of colitis after TNBS induction between days 1 and 6 with observation of stool and measurement of body weight of the rats. The colitis was manifested by diarrhea, appearance of blood in the stool, and loss of weight in the colitis groups in contrast with control group. In the first phase (1–3 days) of acute colitis, the animals demonstrated a significant weight loss relative to the baseline (body weight on day 0) and to the control group. A significant weight gain was observed in the control group and also in the PC-pretreated group, in contrast with the baseline values (Fig. 1).

Hemodynamics

There were no significant changes in the hemodynamic parameters as compared with the baseline values in the sham-operated groups during the observation periods. In series I, MAP values were significantly lower in the colitis group than in the sham-operated group. Phosphatidylcholine feeding normalized this elevation (Fig. 2A). Cardiac output was significantly higher compared with the sham-operated group, and the PC feeding did not influence the colitis-induced changes in

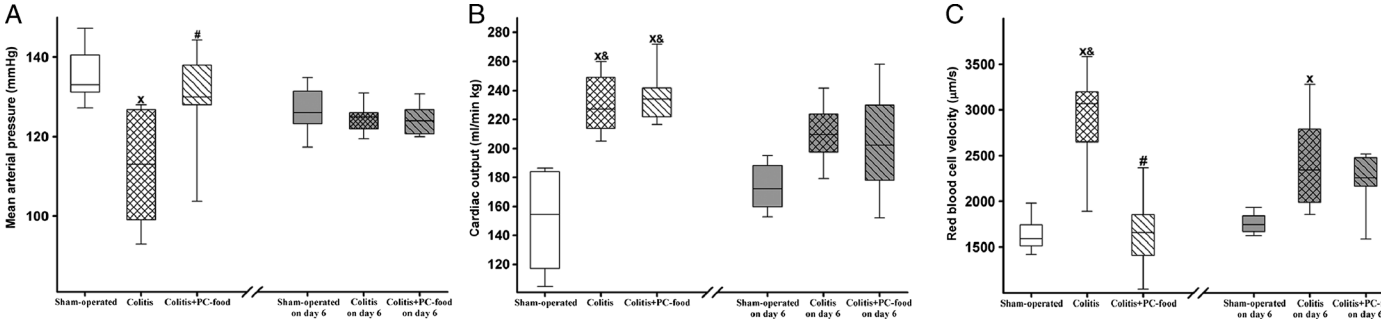

FIG. 2. **Changes in MAP (A), CO (B), and RBCV in colonic serosa (C) on day 1 in the sham-operated (white box), colitis (checked white box), and PC-pretreated colitis (striped white box) groups; and on day 6 in the sham-operated (empty gray box), colitis (checked gray box), and PC-pretreated colitis (striped gray box) groups**. The plots demonstrate the median (horizontal line in the box) and the p25 (lower whisker) and p75 (upper whisker). $^{x}P < 0.05$ between groups and sham-operated group on day 1, $^{\&}P < 0.05$ between groups and sham-operated group on day 6, $^{\#}P < 0.05$ between PC-pretreated group and colitis group on day 1.

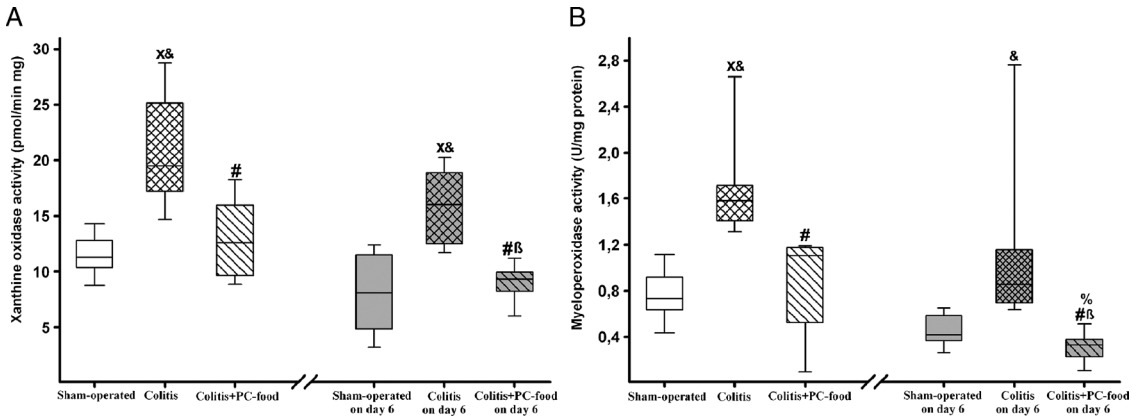

FIG. 3. **Changes in xanthine oxidase activity (A) and MPO activity (B) on day 1 in the sham-operated (white box), colitis (checked white box), and PC-pretreated colitis (striped white box) groups; and on day 6 in the sham-operated (empty gray box), colitis (checked gray box), and PC-pretreated colitis (striped gray box) groups**. The plots demonstrate the median (horizontal line in the box) and the p25 (lower whisker) and p75 (upper whisker). $^{x}P < 0.05$ between groups and sham-operated group on day 1, $^{\&}P < 0.05$ between groups and sham-operated group on day 6, $^{\#}P < 0.05$ between PC-pretreated groups and colitis group on day 1, $^{ß}P < 0.05$ between PC-pretreated groups and colitis group on day 6, $^{\%}P < 0.05$ between PC-pretreated group on day 1 and PC-pretreated group on day 6.

CO as compared with the colitis group (Fig. 2B). There were no significant changes in the HR values in all three groups (data not shown).

In series II, there were no significant differences between the groups in MAP, CO (Fig. 2, A and B), or HR (data not shown) changes 6 days after the vehicle enema or colitis induction.

Microcirculation

The RBCV in the subserosa of the colon was significantly increased on days 1 and 6 of colitis as compared with the sham-operated groups. Phosphatidylcholine administration normalized the colitis-induced elevation in RBCV in series I, but did not cause a significant reduction of RBCV in contrast with the colitis group in series II (Fig. 2C).

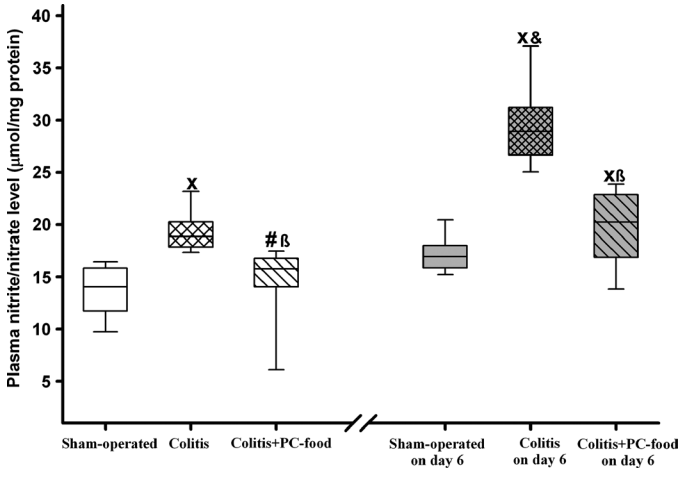

FIG. 4. **Changes in plasma NO_x level on day 1 in the sham-operated (white box), colitis (checked white box), and PC-pretreated colitis (striped white box) groups; and on day 6 in the sham-operated (empty gray box), colitis (checked gray box), and PC-pretreated colitis (striped gray box) groups**. The plots demonstrate the median (horizontal line in the box) and the p25 (lower whisker) and p75 (upper whisker). $^{x}P < 0.05$ between groups and sham-operated group on day 1, $^{\&}P < 0.05$ between groups and sham-operated group on day 6, $^{\#}P < 0.05$ between PC-pretreated groups and colitis group on day 1, $^{ß}P < 0.05$ between PC-pretreated groups and colitis group on day 6.

Biochemical parameters

XOR activity—Mucosal XOR is activated during inflammation processes and produces a considerable amount of superoxide radical. The XOR activity was significantly higher 1 and 6 days after colitis induction as compared with the sham-operated groups. In both cases, the PC-enriched diet effectively decreased the XOR activity in the large bowel in comparison with the nontreated controls (Fig. 3A).

MPO activity—The TNBS enema caused tissue leukocyte accumulation in the proximal colon on days 1 and 6, as determined via the MPO activity. In both cases, PC feeding decreased the MPO activity significantly in the large bowel. In series II, the MPO activity of the PC-treated group was decreased significantly in contrast with the colitis group on day 6 and also with the PC- pretreated group on day 1 (Fig. 3B).

Tissue NO_x levels—In the groups with colitis, a significant elevation in NO_x level was seen in the colonic tissue relative to the controls on day 1. In series II, the elevation of NO_x was significantly higher in comparison with the control group on day 6. Both PC pretreatment protocols decreased the NO_x elevation, in contrast with the nontreated colitis group on day 6, but the NO_x level in the PC-treated group in series II remained significantly higher than that in the sham-operated group on day 1 (Fig. 4).

Changes in plasma TNF-α level—In series I, the plasma level of TNF-α was significantly increased after colitis induction as compared with the control group. In series II, the plasma level of TNF-α was still significantly increased 6 days after colitis induction as compared with the control group. Phosphatidylcholine treatment effectively decreased this change, on day 1 and on day 6 also (Fig. 5A).

Changes in plasma IL-6 level—The plasma IL-6 concentration in the nontreated colitis group was unchanged on day 1 after colitis, but in the PC-pretreated group, an elevated IL-6 level was found. In series II, the IL-6 concentration was significantly increased 6 days after colitis induction relative to the sham-operated group on day 1, to the sham-operated group on day 6 and to the colitis group on day 1. Phosphatidylcholine pretreatment 6 days after colitis induction significantly reduced

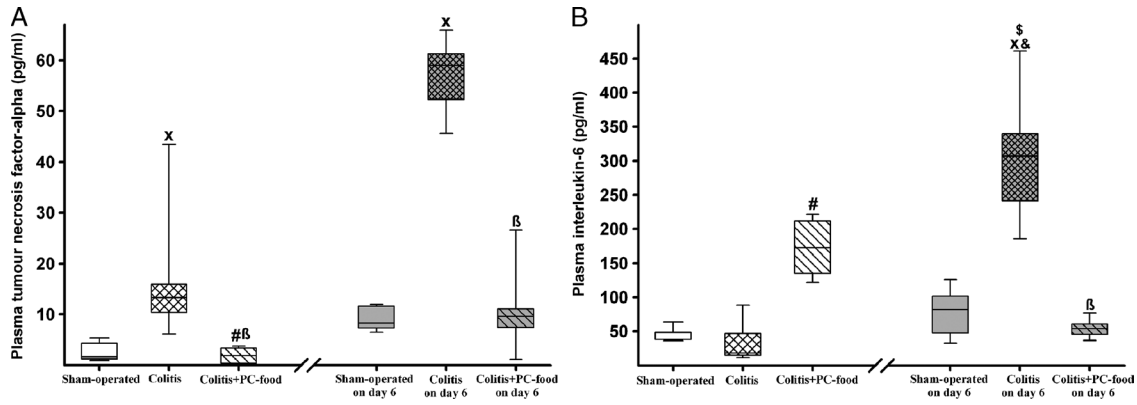

FIG. 5. **Changes in plasma TNF-α (A) and IL-6 (B) levels on day 1 in the sham-operated (white box), colitis (checked white box), and PC-pretreated colitis (striped white box) groups; and on day 6 in the sham-operated (empty gray box), colitis (checked gray box), and PC-pretreated colitis (striped gray box) groups**. The plots demonstrate the median (horizontal line in the box) and the p25 (lower whisker) and p75 (upper whisker). $^{x}P < 0.05$ between groups and sham-operated group on day 1, $^{\&}P < 0.05$ between groups and sham-operated group on day 6, $^{\#}P < 0.05$ between PC-pretreated groups and colitis group on day 1, $^{ß}P < 0.05$ between PC-pretreated groups and colitis group on day 6, $^{\$}P < 0.05$ between colitis group on day 1 and colitis group on day 6.

the plasma IL-6 level in comparison with the colitis group on day 6 (Fig. 5B).

Tissue damage—in vivo *detection*

The colonic microvessels were visualized by FITC-dextran administration, whereas the morphology of the mucosa was examined with the aid of acridine orange staining. In the control group, the luminal openings of the crypts were covered with a continuous layer of epithelial cells, which appeared as black holes opening onto the surface of the mucosa, and the network of capillaries exhibited a honeycomb pattern (mean, 0; p25 = 0; p75 = 0.83; Figs. 6A and 7, A and B). The average number of goblet cells was 1.3 (p25 = 1.2; p75 = 1.4; Fig. 6B).

In series I, the confocal microscopic evaluation demonstrated significant tissue damage in acute phases of colitis (mean, 7.0; p25 = 7.0; p75 = 7.8; Fig. 6A) in contrast with the control groups. The capillary network was disorganized, the honeycomb pattern had disappeared, and fluorescent dye leakage was observed in several areas of the large intestine. A damaged capillary endothelium with edema formation was generally observed (Fig. 7C). The acridine orange staining of the surface of the glands of the mucosa revealed complete loss of the epithelium (Fig. 7D), and the number of goblet cells could not be determined (Fig. 6B).

Phosphatidylcholine feeding significantly influenced both the structural changes in the microvasculature and the epithelial morphology of the inflamed colonic mucosa on day 1 of colitis. These changes were still higher than those in the control group, but the degree of injury was decreased (mean, 4.0; p25 = 4.0; p75 = 4.8; Fig. 6A). The extents of dye leakage and edema formation were diminished, and the loss of epithelium was prevented (Fig. 7, E and F), whereas the number of goblet cells remained at the control level (Fig. 6B).

The tissue damage was also pronounced in the case of subacute colitis, (mean, 4.3; p25 = 2.5; p75 = 5.7; Fig. 6A), in contrast with the sham-operated groups. Fluorescent dye leakage with edema formation was seen in the capillary network, with reduction, thinning, and loss of the epithelium with denuded crypts (Fig. 7G) on the surface of the glands in each case, and the spaces between the glands were greatly enlarged (Fig. 7H). The number of goblet cells was significantly higher relative to day 1 of colitis (Fig. 6B). By day 6, PC pretreatment prevented the structural changes in the microvasculature or the morphology of the inflamed colonic mucosa. The histological

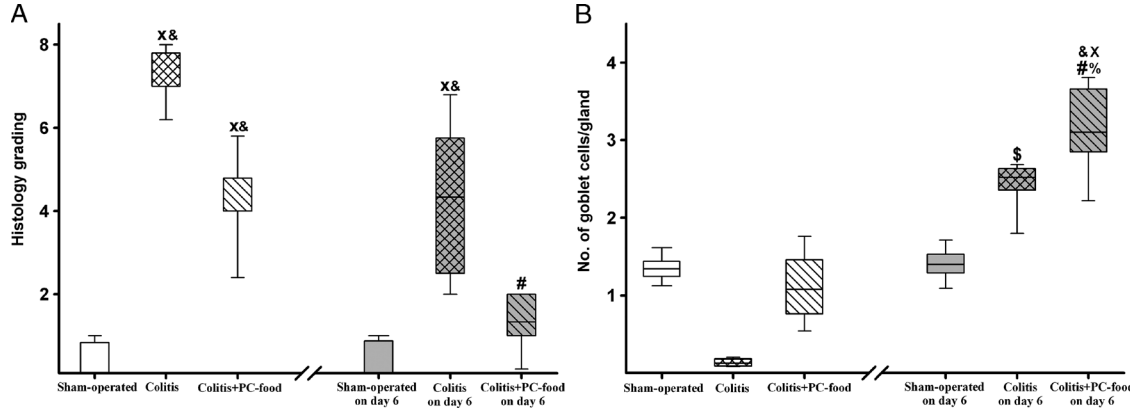

FIG. 6. **Grading of *in vivo* histology (A) and number of goblet cells (B) on day 1 in the sham-operated (white box), colitis (checked white box), and PC-pretreated colitis (striped white box) groups; and on day 6 in the sham-operated (empty gray box), colitis (checked gray box), and PC-pretreated colitis (striped gray box) groups**. The plots demonstrate the median (horizontal line in the box) and the p25 (lower whisker) and p75 (upper whisker). $^{x}P < 0.05$ between groups and sham-operated group on day 1, $^{\&}P < 0.05$ between groups and sham-operated group on day 6, $^{\#}P < 0.05$ between PC-pretreated groups and colitis group on day 1, $^{\$}P < 0.05$ between colitis group on day 1 and colitis group on day 6, $^{\%}P < 0.05$ between PC-pretreated group on day 1 and PC-pretreated group on day 6.

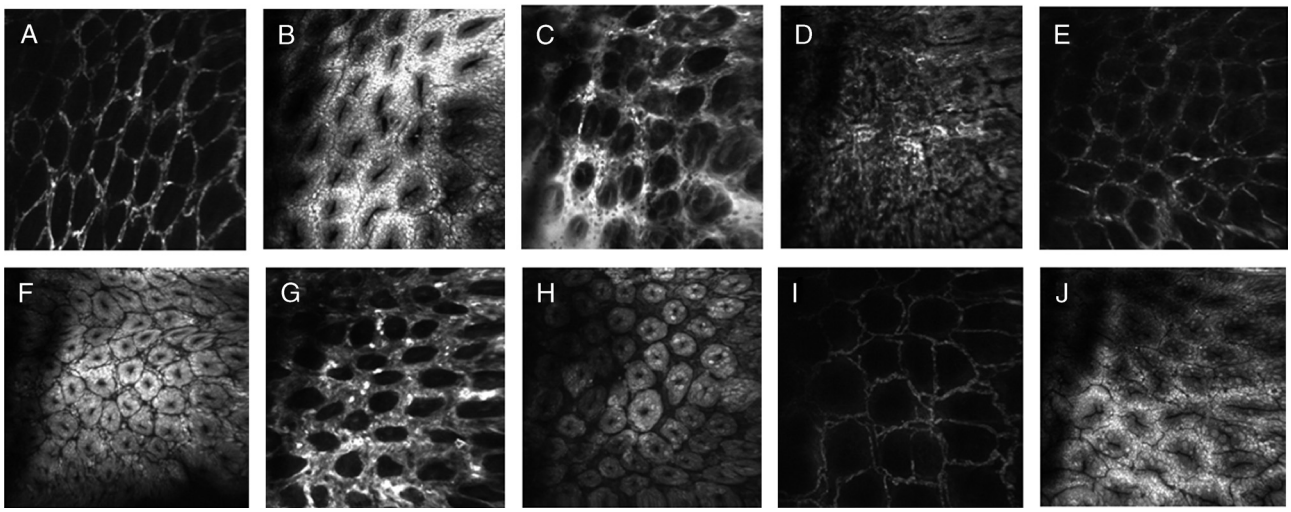

FIG. 7. ***In vivo* histology images of the mucosal surface of the distal rat colon recorded by fluorescence confocal endomicroscopy after intravenous administration of FITC-dextran (A, C, E, G, I) and topical administration of acridine orange (B, D, F, H, J)**. A, Normal mucosal vasculature. B, Normal structure of the mucosa; the luminal openings of the crypts appear as black holes opening onto the surface. C, One day after the TNBS enema, dye leakage from the vessel lumina is observed, and the honeycomb pattern of the capillaries has disappeared. D, Total loss of epithelium on the surface of the glands. E, Moderate dye leakage is observed from the vessel lumina in the PC-pretreated colitis group 1 day after colitis induction. F, The spaces between the glands are enlarged in the PC-pretreated colitis group 1 day after colitis induction. G, Six days after colitis induction, dye leakage is observed from the vessel lumina, and the normal pattern of the capillaries has disappeared. H, Thinning and loss of the epithelium on the surface of the glands; the spaces between the glands are enlarged 6 days after colitis induction. I, The PC-pretreated group with normal mucosal vasculature 6 days after colitis induction. J, The PC-pretreated group with many goblet cells. The luminal openings of the crypts appear as black holes opening onto the surface of the mucosa 6 days after colitis induction.

results indicated decreases in dye leakage and edema. Phosphatidylcholine feeding protected the mucosa from reduction, thinning, and loss of epithelium (Fig. 7, I and J). The changes were significantly lower than those in the sham-operated group on day 1 (mean, 1.3; p25 = 1.0; p75 = 2.0; Fig. 6A). In the PC-pretreated animals, the number of goblet cells was significantly increased in comparison with the sham-operated groups and the PC-pretreated colitis group on day 1 (Fig. 6B).

Conventional light microscopy

Normal colonic mucosal structure was present with no apparent leukocyte infiltration in the control group. Colonic mucosal damage was found in each colitis group, with significant leukocyte infiltration in the nontreated colitis group, whereas the level of leukocyte infiltration was significantly decreased in both PC-treated groups (Fig. 8A).

The grading of histopathological sections revealed a normal colonic mucosal structure in the control group on day 1 and on day 6 (Fig. 8B). No lack of mucin was observed in the colon sections. Colonic mucosal damage was found in both nontreated colitis groups. The mucosal injury on day 1 of colitis involved diffuse transmural damage. Six days after TNBS induction, the damage affected only the lamina propria layer, and the injury was focal. In both nontreated colitis groups, mucin depletion was observed. After pretreatment with PC food, the level of injury was markedly decreased. In both

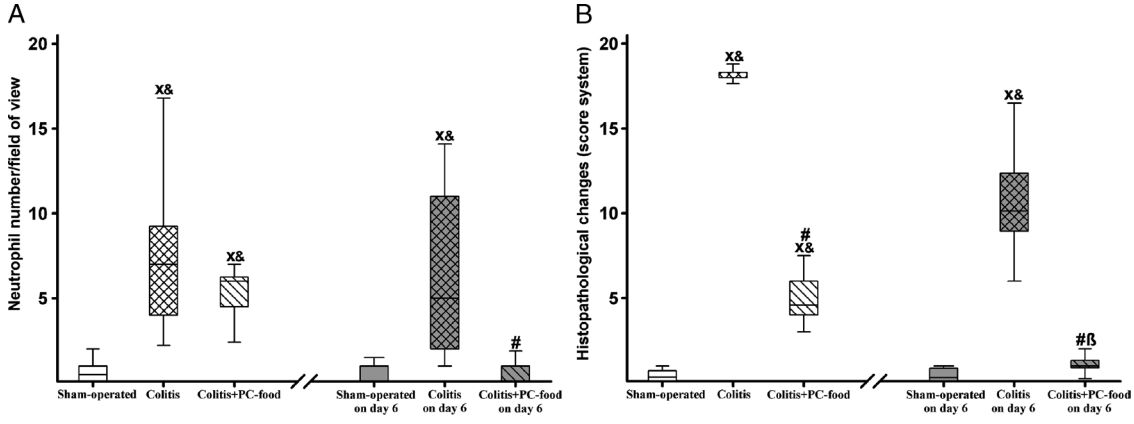

FIG. 8. **Changes in neutrophil leukocyte number/field of view (A) and the grade of histopathological changes (B) on day 1 in the sham-operated (white box), colitis (checked white box), and PC-pretreated colitis (striped white box) groups; and on day 6 in the sham-operated (empty gray box), colitis (checked gray box), and PC-pretreated colitis (striped gray box) groups**. The plots demonstrate the median (horizontal line in the box) and the p25 (lower whisker) and p75 (upper whisker). $^{x}P < 0.05$ between groups and sham-operated group on day 1, $^{\&}P < 0.05$ between groups and sham-operated group on day 6, $^{\#}P < 0.05$ between PC-pretreated groups and colitis group on day 1, $^{ß}P < 0.05$ between PC-pretreated groups and colitis group on day 6.

pretreated groups, PC significantly attenuated the morphologic changes in the inflamed colon, and mucin covered the mucosa.

DISCUSSION

Through the use of intravital techniques, we have demonstrated that dietary PC pretreatment effectively preserves the epithelial and microvascular structure and the number of mucus-producing goblet cells in rats with TNBS-induced experimental colitis. Our data lend support to previous findings and provide new evidence of the beneficial effects of PC supplementation in the GI tract (4, 5, 21). The protective effects of phospholipids in the colon were first outlined after intraluminal application in acetic acid–induced murine colitis (22). Later, polyunsaturated PC mixtures were successfully used in TNBS-provoked colitis (15) and in a double-blind, randomized, placebo-controlled human study. The majority of chronically active IBD patients treated for 3 months with delayed-release PC without concomitant steroid treatment achieved clinical remission or exhibited an improvement of the clinical activity (4).

Our main goals were to characterize the *in vivo* microcirculatory and morphologic changes in the acute and resolving phases of TNBS-induced colitis and to examine the potentially preventive dietary effects of a PC regimen with which to influence such events. The results demonstrate that a PC-enriched diet reduced the signs of colitis-induced local inflammatory activation, normalized the serosal hyperemia, and prevented the epithelial damage to the colonic mucosa. The beneficial histological, hemodynamic, and biochemical changes were already evident after 1 day and also 6 days after the inflammatory challenge.

TNBS-induced colitis is characterized by erosive and self-limiting inflammation, where cellular mechanisms of epithelial cell destruction and repair can be conveniently examined (23). Indeed, intravital confocal laser scanning endomicroscopy revealed the lack of epithelium and complete disruption of the capillary network in the early phase, whereas the morphologic damage was moderate in the resolving phase of colitis; a thinned epithelium and unusually distorted capillary networks were present by day 6. The *in vivo* and real-time histology data revealed the time-dependent differences in epithelial damage and regeneration of the damaged colonic mucosa. By means of this approach, the cellular and subcellular structures of the colonic epithelium (surface epithelium and crypts), connective tissue, and vasculature could be examined. The fluorescent dye leakage presented clear evidence of edema formation, probably the most important indicator of the structural integrity of the microvessels (22) and also of the significantly reduced extravasation in the PC-treated colitis groups.

In addition to the hyperdynamic circulation, serosal hyperemia developed, whereas the later phases of inflammation were accompanied by less colon hyperemia and normalization of the systemic hemodynamics. The activities of the mucosal inflammatory enzymes MPO and XOR were significantly elevated 1 day after the inflammatory challenge, but the increased plasma levels of the proinflammatory cytokines TNF-α and IL-6 persisted even after 6 days. Moreover, the marked leukocyte infiltration was accompanied by biochemical signs of oxidative stress and NO production in the colon.

The serosal microcirculatory hyperemia could be a consequence of the altered synthesis of endothelium-derived mediators, including NO (24), and inducible NO synthase (iNOS)–dependent processes. Inducible NO synthase–derived NO has been implicated in several aspects of the inflammatory cascade in experimental or clinical colitis. We earlier reported that PC treatment inhibited the expression and activity of iNOS isoenzyme *in vivo* (5, 6) and decreased GI tissue NO_x levels in endotoxemic rats (9), and in the present study, PC supplementation significantly decreased the stable end product of NO in the colon tissue in both phases of colitis.

Although the increased PC input clearly conferred protection against excessive epithelial damage in the colon, it is not easy to distinguish the local and systemic effects of the compound. Endogenous PC is an important component of mucosal hydrophobicity and thus contributes to the barrier properties of the epithelium (10, 25, 26). Indeed, it has been shown that the mucus PC concentration and the hydrophobicity of the mucosal surface are significantly reduced after intracolonic TNBS administration (15). More importantly, the total PC and lysophosphatidylcholine concentrations may be significantly reduced in the mucus in the rectum, colon, and terminal ileum of patients with ulcerative colitis (10, 27). The thinner mucus layer cannot separate microorganisms from the mucosa effectively, and thus commensal bacteria will come into direct contact with the epithelial cells (28). Because PC comprises the bulk of phospholipids in the mucus, a selective transport process into the epithelial layer is hypothesized (26). This theory is supported by the results of rat experiments with radiolabeled PC, which demonstrated translocation into the mucus (10, 29). Our observations relating to the increased number of mucus-producing goblet cells in the PC-pretreated colitis groups underline the significance of the PC-induced recovery process in the resolving phase of colitis. As the mucin network is strongly negatively charged, the PC headgroup is bound electrostatically to the mucin network, forming a monolayer with the fatty acid chains extending luminally. This establishes a hydrophobic surface on top of a hydrated gel, which prevents the adherence and penetration of bacteria (21).

Other data suggest that the proportion of more saturated PC species increases under inflammatory conditions, as a consequence of the elevated phospholipase A_2 activity. Decreased PC secretion or an increased breakdown of PC due to elevated epithelial and/or bacterial (30) phospholipase activity can cause a critically low mucus PC concentration (28). On the other hand, a lower adherence of PC to the glycoprotein network due to an altered mucin composition (31) can lead to a critically low mucus PC level and decreased hydrophobicity, especially in the rectum and distal colon (27). This will allow bacteria to adhere directly to the epithelial cells and provoke a mucosal immune response. The nonoccurrence of the protective, anti-inflammatory effect of PC (32), the bacterial colonization, and the activated mucosal immune reaction lead to further deterioration of the mucus.

Another explanation is provided if orally administered PC serves as a slow-release blood choline source, and the choline component of PC is able to influence the inflammatory process through the cholinergic anti-inflammatory pathway (33), including interference with the activation of PMN leukocytes. Nevertheless, the mediators formed during the hydrolysis of PC (e.g., betaine and dimethylglycine) may also influence cell-cell interactions in a favorable manner (34). It was recently found that the multistep extravasation cascade of leukocytes (rolling, adhesion, and transmigration) was reduced by PC in the postischemic periosteum (7). Our present results reveal that PC treatment also decreases the XOR activity and colitis-induced tissue granulocyte accumulation. An elevated XOR activity and PMN accumulation are characteristic of GI inflammation, and the inhibition of PMN leukocyte activation and reduction of the tissue concentrations of PMN- or XOR-derived radicals may therefore result in less tissue damage. In this line, PC metabolites with an alcoholic moiety in the molecule inhibit the reactive oxygen species–producing activity of PMN leukocytes (8, 34). Phosphatidylcholine is readily taken up by phagocytic cells, and accordingly, it may accumulate in inflamed tissues (35). Other *in vitro* data have shown that dipalmitoyl-PC modulates the inflammatory functions of monocytic cells (36) and that a mixture of PC and phosphatidylglycerol inhibits the respiratory burst and superoxide generation of human PMN granulocytes (37). Early reports demonstrated that immunization with PC drastically reduces upregulated TNF-α production in parasitemic mice, in correlation with a shift from a T_H1-type to a protective T_H2-type immune response (38). Indeed, evidence of a TNF-α–linked mechanism of action for PC was provided by recent *in vitro* anti–TNF-α findings and specific inhibition of the TLR-4–dependent inflammatory pathway (39, 40).

The role of TNF-α–induced downregulation of the expression of mucin genes was recently reported in TNBS colitis. Treatment with a TNF-α–neutralizing antibody prevented the depletion of goblet cells and adherent mucin, and through this mechanism, the extent of epithelial cell damage was reduced.[41] Our data also suggest that PC pretreatment protects against elevation of the TNF-α level and increases the count of mucus-producing goblet cells, facilitating the recovery of a protective mucin layer in the later phase of TNBS-induced colitis.

In conclusion, we have presented *in vivo* evidence that dietary PC effectively modulates the inflammatory activation and normalizes the changes in the microcirculation 1 and 6 days after colitis induction. Although the exact mechanism of action is still unclear, the potentially beneficial effects of oral PC supplementation may be linked to the acceleration of the recovery processes of the impaired mucosal barrier.

ACKNOWLEDGMENTS

The authors thank Lipoid KG, Ludwigshafen, Germany, for the generous supply of PC.

REFERENCES

1. Braus NA, Elliott DE: Advances in the pathogenesis and treatment of IBD. *Clin Immunol* 132:1–9, 2009.
2. Rainsford KD: Anti-inflammatory drugs in the 21st century. In Harris RE, ed. *Inflammation in the Pathogenesis of Chronic Diseases. Vol. 42*. The Netherlands: Springer, pp 3–27, 2007.
3. Mourelle M, Guarner F, Malagelada JR: Polyunsaturated phosphatidylcholine prevents stricture formation in a rat model of colitis. *Gastroenterology* 110: 1093–1097, 1996.
4. Stremmel W, Merle U, Zahn A, Autschbach F, Hinz U, Ehehalt R: Retarded release phosphatidylcholine benefits patients with chronic active ulcerative colitis. *Gut* 54:966–971, 2005.
5. Erős G, Kaszaki J, Czobel M, Boros M: Systemic phosphatidylcholine pretreatment protects canine esophageal mucosa during acute experimental biliary reflux. *World J Gastroenterol* 12:271–279, 2006.
6. Erős G, Ibrahim S, Siebert N, Boros M, Vollmar B: Oral phosphatidylcholine pretreatment alleviates the signs of experimental rheumatoid arthritis. *Arthritis Res Ther* 11:43, 2009.
7. Gera L, Varga R, Torok L, Kaszaki J, Szabo A, Nagy K, Boros M: Beneficial effects of phosphatidylcholine during hindlimb reperfusion. *J Surg Res* 139:45–50, 2007.
8. Ghyczy M, Torday C, Kaszaki J, Szabo A, Czobel M, Boros M: Oral phosphatidylcholine pretreatment decreases ischaemia-reperfusion–induced methane generation and the inflammatory response in the small intestine. *Shock* 30:596–602, 2008.
9. Tőkés T, Erős G, Bebes A, Hartmann P, Várszegi Sz, Varga G, Kaszaki J, Gulya K, Ghyczy M, Boros M: Protective effects of a phosphatidylcholine-enriched diet in lipopolysaccharide-induced experimental neuroinflammation in the rat. *Shock* 36:458–465, 2011.
10. Ehehalt R, Wagenblast J, Erben G, Lehmann WD, Hinz U, Merle U, Stremmel W: Phosphatidylcholine and lysophosphatidylcholine in intestinal mucus of ulcerative colitis patients. A quantitative approach by nanoelectrospray–tandem mass spectrometry. *Scand J Gastroenterol* 39:737–742, 2004.
11. Neurath MF, Fuss I, Pasparakis M, Alexopoulou L, Haralambous S, Meyer zum Büschenfelde KH, Strober W, Kollias G: Predominant pathogenic role of tumor necrosis factor in experimental colitis in mice. *Eur J Immunol* 27: 1743–1750, 1997.
12. Kiss J, Lamarque D, Delchier JC, Whittle BJR: Time-dependent actions of nitric oxide synthase inhibition on colonic inflammation induced by trinitrobenzene sulphonic acid in rats. *Eur J Pharmacol* 336:219–224, 1997.
13. Yue G, Lai PS, Yin K, Sun FF, Nagele RG, Liu X, Linask KK, Wang C, Lin KT, Wong PYK: Colon epithelial cell death in 2,4,6-trinitrobenzenesulfonic acid-induced colitis is associated with increased inducible nitric-oxide synthase expression and peroxynitrite production. *J Pharmacol Exp Ther* 297:915–925, 2001.
14. Morris GP, Beck PL, Herridge MS, Depew WT, Szewczuk MR, Wallace JL: Hapten-induced model of chronic inflammation and ulceration in the rat colon. *Gastroenterology* 96:795–803, 1989.
15. Tatsumi Y, Lichtenberger LM: Molecular association of trinitrobenzenesulfonic acid and surface phospholipids in the development of colitis in rats. *Gastroenterology* 110:780–789, 1996.
16. Deban L, Correale C, Vetrano S, Malesci A, Danese S: Multiple pathogenic roles of microvasculature in inflammatory bowel disease: a jack of all trades. *Am J Pathol* 172:1457–1466, 2008.
17. Vermeulen W, De Man J, Nullens S, Pelckmans PA, De Winter BY, Morrels TG: The use of colonoscopy to follow the inflammatory time course of TNBS colitis in rats. *Acta Gastroenterol Belg* 74:304–311, 2011.
18. McLaren WJ, Anikijenko P, Thomas SG, Delaney PM, King RG: *In vivo* detection of morphological and microvascular changes of the colon in association with colitis using fiberoptic confocal imaging (FOCI). *Dig Dis Sci* 47:2424–2433, 2002.
19. Kiesslich R, Goetz M, Angus EM, Hu Q, Guan Y, Potten C, Allen T, Neurath M, Shroyer N, Montrose MH, Watson AJM: Identification of epithelial gaps in human small and large intestine by confocal endomicroscopy. *Gastroenterology* 133:1769–1778, 2007.
20. Riley SA, Mori V, Goldman MJ, Dutt S, Herd ME: Microscopic activity in ulcerative colitis: what does it mean? *Gut* 32:174–178, 1991.
21. Lichtenberger LM: The hydrophobic barrier properties of gastrointestinal mucus. *Annu Rev Physiol* 57:565–583, 1995.
22. Fabia R, Ar'Rajab A, Willen R, Andersson R, Ahren B, Larsson K, Bengmark S: Effects of phosphatidylcholine and phosphatidylinositol on acetic-acid-induced colitis in the rat. *Digestion* 53:35–44, 1992.
23. Grisham MB: Do different animal models of IBD serve different purposes? *Inflamm Bowel Dis Suppl* 2:132–133, 2008.
24. Hatoum OA, Binion DG, Otterson MF, Gutterman DD,: Acquired microvascular dysfunction in inflammatory bowel disease: loss of nitric oxide–mediated vasodilation. *Gastroenterology* 125:58–69, 2003.
25. Ehehalt R, Braun A, Karner M, Füllekrug J, Stremmel W: Phosphatidylcholine as a constituent in the colonic mucosal barrier—physiological and clinical relevance. *Biochim Biophys Acta* 1801:983–993, 2010.

26. Stremmel W, Hanemann A, Ehehalt R, Karner M, Braun A: Phosphatidylcholine (Lecithin) and the mucus layer: evidence of therapeutic efficacy in ulcerative colitis? *Dig Dis* 28:490–496, 2010.
27. Braun A, Treede I, Gotthardt D, Tietje A, Zahn A, Ruhwald R, Schoenfeld U, Welsch T, Kienle P, Erben G, et al.: Alterations of phospholipid concentration and species composition of the intestinal mucus barrier in ulcerative colitis: a clue to pathogenesis. *Inflamm Bowel Dis* 15:1705–1720, 2009.
28. Swidsinski A, Ladhoff A, Pernthaler A, Swidsinski S, Loening-Baucke V, Ortner M, Weber J, Hoffmann U, Schreiber S, Dietel M, et al.: Mucosal flora in inflammatory bowel disease. *Gastroenterology* 122:44–54, 2002.
29. Dial EJ, Zayat M, Lopez-Storey M, Tran D, Lichtenberger L: Oral phosphatidylcholine preserves the gastrointestinal mucosal barrier during LPS-induced inflammation. *Shock* 30:729–733, 2008.
30. Mauch F, Bode G, Ditschuneit H, Malfertheiner P; Demonstration of a phospholipid-rich zone in the human gastric epithelium damaged by *Helicobacter pylori*. *Gastroenterology* 105:1698–1704, 1993.
31. Einerhand AW, Renes IB, Makkink MK, van der Sluis M, Buller HA, Dekker J: Role of mucins in inflammatory bowel disease: important lessons from experimental models. *Eur J Gastroenterol Hepatol* 14:757–765, 2002.
32. Treede I, Braun A, Sparla R, Kuhnel M, Giese T, Turner JR, Anes E, Kulaksiz H, Fullekrug J, Stremmel W, et al.: Anti-inflammatory effects of phosphatidylcholine. *J Biol Chem* 282:27155–27164, 2007.
33. Tracey KJ: Physiology and immunology of the cholinergic antiinflammatory pathway. *J Clin Invest* 117:289–296, 2007.
34. Ghyczy M, Torday C, Boros M: Simultaneous generation of methane, carbon dioxide, and carbon monoxide from choline and ascorbic acid—a defensive mechanism against reductive stress? *FASEB J* 17:1124–1126, 2003.
35. Miranda DTSZ, Batista VG, Grando FCC, Paula FMP, Felício CA, Rubbo GFS, Fernandes LC, Curi R, Nishiyama A: Soy lecithin supplementation alters macrophage phagocytosis and lymphocyte response to concanavalin A: a study in alloxan-induced diabetic rats. *Cell Biochem Funct* 26:859–865, 2008.
36. Tonks A, Morris RH, Price AJ, Thomas AW, Jones KP, Jackson SK: Dipalmitoylphosphatidylcholine modulates inflammatory functions of monocytic cells independently of mitogen activated protein kinases. *Clin Exp Immunol* 124:86–94, 2001.
37. Chao W, Spragg RG, Smith RM: Inhibitory effect of porcine surfactant on the respiratory burst oxidase in human neutrophils. Attenuation of p47phox and p67phox membrane translocation as the mechanism. *J Clin Invest* 96: 2654–2660, 1995.
38. Bordmann G, Rudin W, Favre N: Immunization of mice with phosphatidylcholine drastically reduces the parasitaemia of subsequent *Plasmodium chabaudi* blood-stage infections. *Immunology* 94:35–40, 1998.
39. Treede I, Braun A, Jeliaskova P, Giese T, Füllekrug J, Griffiths G, Stremmel W, Ehehalt R: TNF-alpha–induced up-regulation of pro-inflammatory cytokines is reduced by phosphatidylcholine in intestinal epithelial cells. *BMC Gastroenterol* 9:53, 2009.
40. Ishikado A, Nishio Y, Yamane K, Mukose A, Morino K, Murakami Y, Sekine O, Makino T, Maegawa H, Kashiwagi A: Soy phosphatidylcholine inhibited TLR4-mediated MCP-1 expression in vascular cells. *Atherosclerosis* 205:404–412, 2009.
41. Dharmani P, Leung P, Chadee K: Tumor necrosis factor-α and Muc2 mucin play major roles in disease onset and progression in dextran sodium sulphate-induced colitis. *PLoS One* 6:e25058, 2011.